Article

# Interactions of Macromolecular Crowding Agents and Cosolutes with Small-Molecule Substrates: Effect on Horseradish Peroxidase Activity with Two Different Substrates

William M. Aumiller, Jr., Bradley W. Davis, Emmanuel Hatzakis, and Christine D. Keating*

Department of Chemistry, The Pennsylvania State University, University Park, Pennsylvania 16802, United States

S Supporting Information

**ABSTRACT:** The importance of solution composition on enzymatic reactions is increasingly appreciated, particularly with respect to macromolecular cosolutes. Macromolecular crowding and its effect on enzymatic reactions has been studied for several enzymes and is often understood in terms of changes to enzyme conformation. Comparatively little attention has been paid to the chemical properties of small-molecule substrates for enzyme reactions in crowded solution. In this article, we studied the reaction of horseradish peroxidase (HRP) with two small-molecule substrates that differ in their hydrophobicity. Crowding agents and cosolutes had quite different effects on HRP activity when the substrate used was 3,3′,5,5′-tetramethylbenzidine (TMB, which is hydrophobic) as compared to o-phenylenediamine (OPD, which is more hydrophilic). Reaction rates with TMB were much more sensitive to the presence of crowding agents and cosolutes than OPD, suggesting that the small-molecule substrates may themselves be interacting with crowders and cosolutes. At high polyethylene glycol (PEG) concentrations (25−30 wt/wt %), no reaction was observed for TMB. Even at lower concentrations, Michaelis constants ($K_M$) for HRP with the more hydrophobic substrate increased in the presence of crowding agents and cosolutes, particularly with PEG. Diffusion of TMB and OPD in the PEG and dextran reaction media was evaluated using pulsed field gradient nuclear magnetic resonance (PFG-NMR). The diffusivity of the TMB decreased 3.9× in 10% PEG 8k compared to that in buffer and decreased only 1.7× for OPD. Together, these data suggest that weak attractive interactions between small-molecule substrates and crowders or cosolutes can reduce substrate chemical activity and consequently decrease enzyme activity and that these effects vary with the identity of the molecules involved. Because many enzymes can act on multiple substrates, it is important to consider substrate chemistry in understanding enzymatic reactions in complex media such as biological fluids.
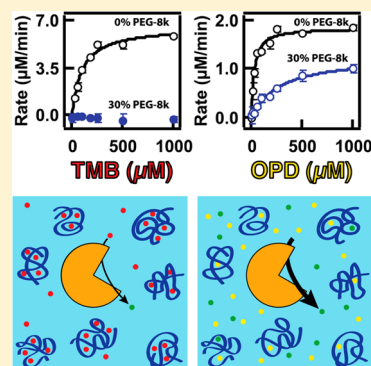
## INTRODUCTION

The cytoplasm of biological cells is composed of approximately 30% by volume biomacromolecules such as proteins, nucleic acids, and polysaccharides.[1,2] This environment differs from the idealized dilute buffer solutions in which enzymes are often studied.[2−6] The effects of macromolecular crowding on enzymatic reactions are becoming increasingly realized with reports of enhanced rates of reaction,[2,7−12] some with loss of activity,[12−15] or little to no changes.[16] Substrate-dependent effects of crowding agents and cosolutes on enzyme activity are generally not considered. The possibility of substrate-dependent differences in the effects of crowding on enzyme activity warrants investigation because many enzymes act on multiple substrates in vivo,[17] and for ease of analysis, many enzymes are routinely assayed using non-native substrates.[18,19] In this article, the activity of horseradish peroxidase (HRP) with respect to two different commonly used substrates is investigated in the presence of background macromolecular crowding agents and cosolutes.

The volume exclusion aspect of macromolecular crowding has been widely studied for many proteins and nucleic acids.[2] For associative interactions of proteins and nucleic acids, the effects of excluded volume alone will favor more compact structures.[2,20] Changes in enzyme activity in the presence of crowding agents are often ascribed to changes in enzyme conformation.[21] For example, Pozdnyakova and Wittung-Stafshede report that for the enzyme multicopper oxidase, a weaker binding of the substrate was observed and may be explained by the active site adopting a more rigid conformation, restricting substrate binding.[14] At higher concentration of crowding agent, a decrease in the Michaelis constant, $K_M$, was observed, possibly due to an increase in the effective concentration of the enzyme and substrate. In another example, a conformational change in the enzyme isochorismate synthase (EntC) was observed in Ficoll solution, which resulted in a decrease in the $K_M$ of the substrate.[22] There are other factors that may affect the kinetics of an enzyme in crowded solution, such as reduced and/or anomalous diffusion[23,24] and the activity of water.[25,26] Therefore, it is difficult to predict a priori for a particular enzymatic reaction of interest the kinetic effects of macromolecular crowding.

The chemical effects of macromolecular crowding have only begun to be realized in the past decade. Chemical interactions between a solute and the other species in solution can be repulsive, resulting in increased chemical activity for the solute or attractive, which decreases its chemical activity. For macromolecules such as proteins or DNA, repulsive interactions with background molecules will enhance the effects of volume exclusion. Attractive interactions, however, often lead to a more destabilized structure and can promote unfolding;[27,28] the protein chymotrypsin inhibitor 2 was recently shown to be destabilized in reconstituted *E. coli* cytosol despite the excluded volume ($\geq$100g/L macromolecules).[29] Typically, chemical effects of macromolecular crowding are only investigated with respect to the effect on other macromolecules, but small-molecule substrates could potentially experience attractive or repulsive interactions with the background macromolecules.[30] The phenomenon known as substrate channeling occurs when an intermediate is transferred from one enzyme active site to another without diffusing in the bulk solvent.[31] While some examples of this are more due to steric constraints like tryptophan synthase (where the hydrophobic substrate indole is transferred by means of a hydrophobic tunnel),[32] others like dihydrofolate reductase-thymidylate synthase transfer the negatively charged substrate dihydrofolate by means of electrostatic interaction with positively charged residues in the enzymes.[33] Record and co-workers separated the chemical effects from the volume exclusion effects of PEG on DNA structure. They showed that attractive interactions between DNA and small molecular weight PEGs led to destabilization of DNA hairpin and duplex formation.[34] Often, researchers will use a particular small-molecule substrate so that the effects of macromolecular crowding (more specifically, excluded volume) on the substrate can be ignored because it does not occupy much volume compared to the macromolecules;[13,15] however, this neglects any chemical interactions that may be present between the substrates and crowders.

In addition to crowded solutions of large macromolecular solutes, small-molecule cosolutes/osmolytes can alter enzyme kinetics. In general, compatible osmolytes have a stabilizing effect on protein structure because of their exclusion from the protein−water interface, which promotes a more compact, folded structure;[35−37] osmolytes may enhance or decrease enzyme activity.[38] For example, hexokinase activity was decreased in the presence of glycerol, was increased in the presence of betaine and urea solution, and was not significantly affected in trimethylamine N-oxide (TMAO).[38] Although the osmolytes with the exception of urea are expected to be excluded from the enzyme surface, the authors suggest that some type of interaction with the hexokinase caused the activity to change. Recent work by Howell and co-workers indicates the possibility of osmolytes interacting with small-molecule substrates through weak binding interactions. They report preferential interactions of folate (a model compound for dihydrofolate reductase, substrate dihydrofolate) with osmolytes betaine and dimethyl sulfoxide (DMSO).[39] Like macromolecular crowders, the effects of cosolute interactions also cannot easily be predicted.

We report the significant effects of various macromolecular crowding agents (polyethylene glycol (PEG) 8k, dextran 10k) and cosolutes (PEG 400 and glucose) on the reaction of HRP. We analyzed the effect of the different crowding agents and cosolutes on the $K_M$ and the maximal velocity ($V_{max}$) of two substrates, *o*-phenylenediamine (OPD) and 3,3′,5,5′-tetrame-

thylbenzidine (TMB). These substrates were chosen due to their different hydrophobic properties. We reasoned that due to the relative hydrophilic/hydrophobic nature of the background molecules, we would observe various effects on enzymatic activity due to interactions between the background macromolecules and the substrates. We found that the effect on the kinetics was modest for the OPD substrate but substantial for the TMB reaction, especially with respect to the relatively more hydrophobic crowder, PEG 8k. We also measured the diffusion coefficients of the OPD and TMB in buffer, 10% PEG 8k and 10% dextran 10k solutions using pulsed field gradient nuclear magnetic resonance (PFG-NMR). The presence of PEG decreased the diffusion coefficient for TMB disproportionately as compared with OPD. This suggests that weak attractive interactions between the more hydrophobic TMB and the PEG are responsible for the different impact of this crowder on HRP reaction rates with the two substrates.

## ■ RESULTS AND DISCUSSION

HRP activity is commonly used as a reporter in an enzyme-linked immunosorbent assay (ELISA) and other types of bioassays due to its stability and the ease of detecting its products.[40] HRP can oxidize many different aromatic substrates, which made it possible for us to select two common substrates for comparison in this investigation. We had previously measured HRP kinetics as part of a coupled reaction in a PEG/sodium citrate aqueous two-phase system (ATPS).[41] HRP activity toward its substrate Amplex Red in the more hydrophobic PEG-rich phase was decreased substantially as compared to the citrate-rich phase. Indeed, kinetics in the PEG-rich phase could not be fit with the standard Michaelis−Menten equation because the rate increased linearly up to the point of substrate solubility. This observation, coupled with Amplex Red's strong partitioning preference for the PEG-rich phase of the ATPS, suggested to us that there could be an attractive interaction between the substrate and the PEG leading to decreased availability of the Amplex Red.

For the present study, we chose two chemically distinct substrates, OPD and TMB, to evaluate whether substrate−crowder interactions could be important. The value log $D$ is a measure of the partitioning of a compound with ioniziable functional groups in a water−octanol system, and it serves to gauge the relative lipophilicity (hydrophilicity/hydrophobicity) of a small molecule. Compounds with log $D > 0$ partition to the octanol phase of a water−octanol system and are more lipophilic. OPD is highly water-soluble and one of the least hydrophobic HRP substrates (log $D$ at pH 7 = 0.24);[42] TMB is sparingly water-soluble and one of the most hydrophobic substrates (log $D$ at pH 7 = 2.67)[43] (Chart 1). The OPD reaction was monitored by the absorbance of the product 2,3-diaminophenazine (DAP). The TMB reaction was monitored using the diamine/diimine charge-transfer complex. We verified that the established extinction coefficients for these products

**Chart 1. Substrates Used in This Work**



*o*-phenylenediamine
(OPD)
log D = 0.24

3,3',5,5'-tetramethylbenzidine
(TMB)
log D = 2.67
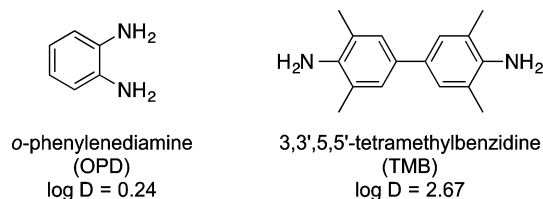
were valid in the complex media used here (see the Experimental Section).[44] PEG was chosen as a crowding agent and as a small-molecule cosolute in these experiments because it has been widely used as a crowding agent and is known to have interactions with hydrophobic molecules[45] and with hydrophobic portions of proteins.[2] Dextran 10k was chosen because it is a commonly used crowding agent. The buffer used in this work was 50 mM sodium phosphate, pH 7.4, with 1 mM EDTA added to complex any trace metal ions that may cause background oxidation of the small-molecule substrates.

**HRP Activity, $K_M$ of Substrates in Macromolecular Crowding Agents.** We first measured the effect of crowding on HRP reaction kinetics for the OPD and TMB substrates in solutions of the macromolecular crowding agents, PEG 8k and dextran 10k, (Figure 1, additional crowder concentrations in
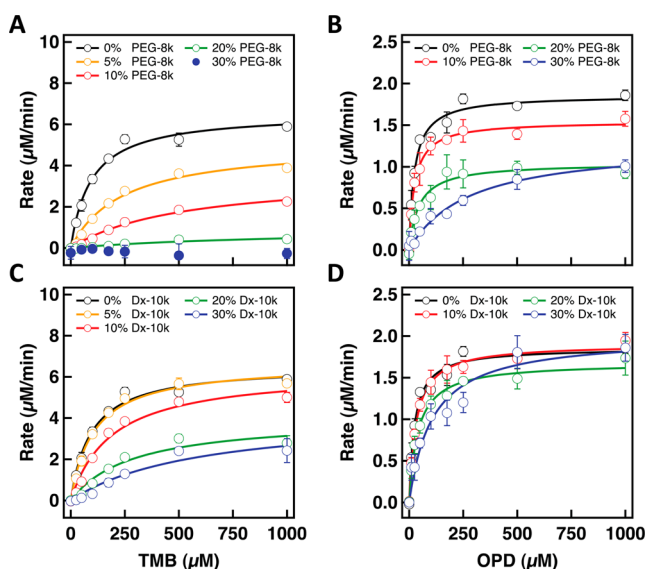


**Figure 1.** Michaelis−Menten plots of the reaction of HRP with TMB and OPD in different crowding agents. (A) TMB in PEG 8k; (B) OPD in PEG 8k; (C) TMB in dextran 10k; (D) OPD in dextran 10k; The HRP concentration was 0.005 U/mL (0.45 nM) for all assays. The data points are the average of three measurements with standard deviation error bars. The traces are the fit to the standard Michaelis−Menten equation. TMB data for 30% PEG 8k could not be fit to the equation.

Supporting Information Figure 1). Data were fit with the Michaelis−Menten equation; Table 1 summarizes $K_M$ and $V_{max}$ values for each set of conditions. In all cases, $K_M$ increased as the weight percent of the crowding agent increased; however, the effects were different both between crowders for the same substrate and between substrates for the same crowder. For TMB, $K_M$ increased more than 2-fold in just 5% and more than 10-fold in 20% PEG 8k. Above 25% PEG 8k, the reaction of HRP with TMB was essentially shut down, and data could not be fit with Michaelis−Menten kinetics. PEG 8k also increased the $K_M$ for OPD but only at higher concentrations of crowding agent. At 10% PEG 8k, $K_M$ for OPD was the same as that without crowder, while by 30% PEG, it had increased more than 10-fold. Dextran also increased $K_M$ for both substrates but to a lesser degree than PEG. At 30% dextran, the $K_M$ for TMB increased 6-fold, while the $K_M$ for OPD increased nearly 3-fold.

An increase in $K_M$ can been attributed to changes in the active site of an enzyme.[13] We cannot rule out this contribution

to the increase in $K_M$ as substrate access can be hindered by changes in the local protein environment of HRP.[46] However, we expect that the local protein environment in the crowding agents would be the same regardless of the substrate used. Another study reported that dextran had little effect on HRP $K_M$ using the substrate 2,2′-azino-bis(3-ethylbenzothiazoline-6-sulfonic acid) (ABTS), observing a small decrease that was not statistically different compared to the $K_M$ in buffer.[47] ABTS is more hydrophilic than OPD, with log $D = -3.59$ at pH 7;[48] therefore, it is not surprising that the $K_M$ was not changed in dextran. In our previous work using Amplex Red, with log $D = 1.94$,[49] HRP activity could not be fit to Michaelis−Menten kinetics,[41] which is also consistent with this hydrophobic substrate interacting with the PEG. An increase in $K_M$ may also be caused by increased diffusion resistance within the sample.[13,50] While an increase in viscosity due to the crowding agents could account for some of the observed decrease in enzyme kinetics, it cannot account for the much larger changes that we observed in $K_M$ and $V_{max}$ for the TMB substrate as compared with the OPD substrate. These substrates have similar molecular weights (OPD $M_w = 108.14$ Da; TMB $M_w = 240.34$ Da); therefore, we would expect the diffusivity of both substrates to decrease similarly if viscosity was the only factor affecting the diffusion; that was not observed here. Experimentally determined viscosities for weight percents of crowding agent and cosolute at 17 °C (lab temperature used in enzyme assays) and 25 °C (temperature of NMR experiments) are compiled in Supporting Information Table 1.

**$V_{max}$ Analysis in Macromolecular Crowding Agents.** The $V_{max}$ of the substrates was either statistically unchanged or decreased with respect to increasing weight percent of the crowding agents. For OPD, $V_{max}$ decreased slightly in the PEG 8k and was essentially unchanged with respect to buffer in dextran 10 kDa. For TMB, $V_{max}$ decreased steadily in PEG 8k until there was no reaction and decreased slightly in dextran 10k.

A decrease in $V_{max}$ has usually been attributed to a change in the active site of the enzyme by the environmental surroundings.[21,51] Other studies report crowding effects on HRP activity. Altikatoglu and Basaran studied the reaction with respect to the substrate o-dianisidine in various molecular weights of dextran and found that the activity was decreased in dextran 17.5k compared to that in buffer, curiously was increased ∼2-fold in dextran 75k, and then decreased as the molecular weight of the dextran increased.[52] Pitulice et al. measured the rate with respect to ABTS and also found that the $V_{max}$ was decreased,[47] as we observed here. These studies and our work point to a general volume exclusion effect that is changing the enzyme active site. Aromatic substrates bind to HRP by a solvent-exposed heme edge that has an active site composed of flexible amino acids; it can accommodate many different small aromatic molecules.[53] Volume exclusion could cause a conformation change that is sterically restricting access to the active site. Polymer−protein interactions[27,54,55] can also be restricting substrate access. As described above, this may contribute to the macromolecular crowding effect that we and others observe but cannot adequately explain that the $V_{max}$ decreased to zero for the TMB substrate and only slightly decreased or stayed the same for the OPD substrate under the same HRP crowding conditions.

**HRP Activity in the Presence of Small Molecule Cosolutes.** To further investigate potential chemical interactions with the media without the excluded volume effects of

**Table 1. Michaelis−Menten Reaction Parameters for TMB and OPD in the Various Macromolecular Crowding Agents[a]**

| | | TMB | | OPD | |
|---|---|---|---|---|---|
| media | wt % | $K_M$ ($\mu$M) | $V_{max}$ ($\mu$M/min) | $K_M$ ($\mu$M) | $V_{max}$ ($\mu$M/min) |
| buffer | 0 | 100 ± 10 | 6.6 ± 0.3 | 25 ± 4 | 1.86 ± 0.06 |
| PEG 8k | 5 | 240 ± 40 | 5.1 ± 0.4 | | |
| | 10 | 500 ± 100 | 3.5 ± 0.4 | 26 ± 3 | 1.55 ± 0.03 |
| | 15 | 1100 ± 500 | 2.5 ± 0.7 | | |
| | 20 | 1100 ± 800 | 1.0 ± 0.5 | 45 ± 9 | 1.04 ± 0.05 |
| | 25 | na | na | | |
| | 30 | na | na | 280 ± 50 | 1.28 ± 0.10 |
| dextran 10k | 5 | 110 ± 10 | 6.7 ± 0.3 | | |
| | 10 | 190 ± 40 | 6.3 ± 0.5 | 38 ± 3 | 1.90 ± 0.04 |
| | 15 | 210 ± 70 | 5.3 ± 0.6 | | |
| | 20 | 300 ± 100 | 4.0 ± 0.6 | 36 ± 3 | 1.68 ± 0.05 |
| | 25 | 600 ± 200 | 5 ± 1 | | |
| | 30 | 600 ± 300 | 4 ± 1 | 70 ± 10 | 2.0 ± 0.2 |

[a]na: Not applicable. That data could not be fit with Michaelis−Menten kinetics.

the polymers, we used PEG 400 and glucose as cosolutes and conducted each of the reactions in solution up to 30 wt % (Figure 2, Table 2, Supporting Information Figure 1). HRP
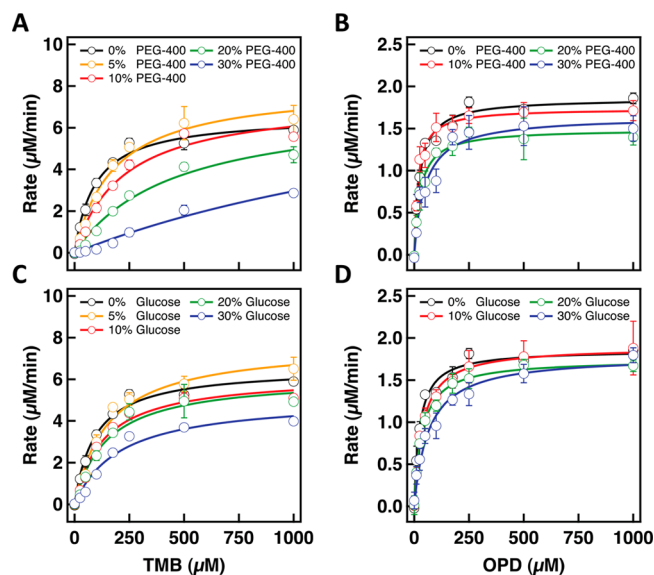


**Figure 2.** Michaelis−Menten plots of the reaction of HRP with OPD and TMB in different cosolutes. (A) TMB in PEG 400; (B) OPD in PEG 400; (C) TMB in glucose; (D) OPD in glucose. The HRP concentration was 0.005 U/mL (0.45 nM) for all assays. The data points are the average of three measurements with standard deviation error bars. The traces are the fit to the standard Michaelis−Menten equation.

kinetics were not substantially changed with respect to the OPD substrate in either cosolute. For the TMB substrate, however, $K_M$ was increased substantially. This is consistent with a chemical interaction between the TMB substrate and the PEG 400, as was observed with the PEG 8k. With TMB, the $K_M$ in glucose also increased but increased to a much smaller extent than that for PEG 400, similar to the larger effect of PEG 8k than dextran in Figure 1. Together, these data for small molecules suggest that chemical interactions are important for understanding the differences between the two small-molecule substrates. The larger effects seen for macromolecular cosolutes also indicate that excluded volume effects account for some of

the observed changes in HRP kinetics as compared with reactions performed in buffer.

**Diffusion Coefficients of OPD and TMB in Different Media.** PFG-NMR was used to measure the impact of the PEG 8 kDa and dextran 10 kDa crowders on OPD and TMB diffusion coefficients. When translational diffusion of small molecules is reduced due to interactions with polymers in solution, this can be measured using PFG-NMR.[56−59] We measured the diffusion coefficient, $D$, of OPD and TMB together in buffer alone, 10% PEG 8k, and 10% dextran 10k. This crowder concentration was chosen because a difference in enzyme activity was observed at 10%, and higher polymer concentrations are more challenging for NMR diffusion experiments. A schematic way to view the diffusion data is the diffusion ordered NMR (DOSY) representation where the signal attenuation at each chemical shift is inverted by an approximate inverse Laplace transformation (ILT). The DOSY representation of the data is presented as a 2D spectrum with chemical shifts on the horizontal axis and the distribution of the diffusion coefficients on the vertical axis shown in Figure 3. The individual 1D $^1$H spectra are also included for buffer, 10% PEG, and 10% dextran.

Diffusion coefficients for each substrate in buffer, 10% PEG 8k, and 10% dextran 10k are given in Table 3. The coefficients were calculated using eq 2 (see the Experimental Section). $D_{OPD,PEG}$ decreased by a factor of 1.7 compared to $D_{OPD,buffer}$, and the $D_{TMB,PEG}$ decreased by a factor of 3.9. For dextran, the diffusion coefficients decreased by a similar factor. $D_{OPD,dex}$ decreased 1.6× compared to buffer, while $D_{TMB,dex}$ decreased 2.3× compared to buffer.

We expect that the diffusion coefficients would decrease due to the increased viscosity of these solutions, as anticipated by the Stokes−Einstein equation, which can provide a first-order estimate of a diffusion coefficient.[60] Diffusion coefficients do not always scale proportionally with viscosity in liquids because diffusion reflects short-range interactions while viscosity often depends on longer-range interactions in the solution.[61] The larger decrease in the diffusion coefficient of TMB in PEG versus OPD in PEG suggests that there is an interaction between the TMB and PEG that is either smaller or not present between OPD and PEG. The fold-decrease for the OPD and TMB in dextran was not identical but was more similar in magnitude than that for OPD and TMB in PEG. The change in diffusion that we observe for OPD and TMB can

**Table 2. Michaelis−Menten Reaction Parameters for TMB and OPD in the Cosolutes**

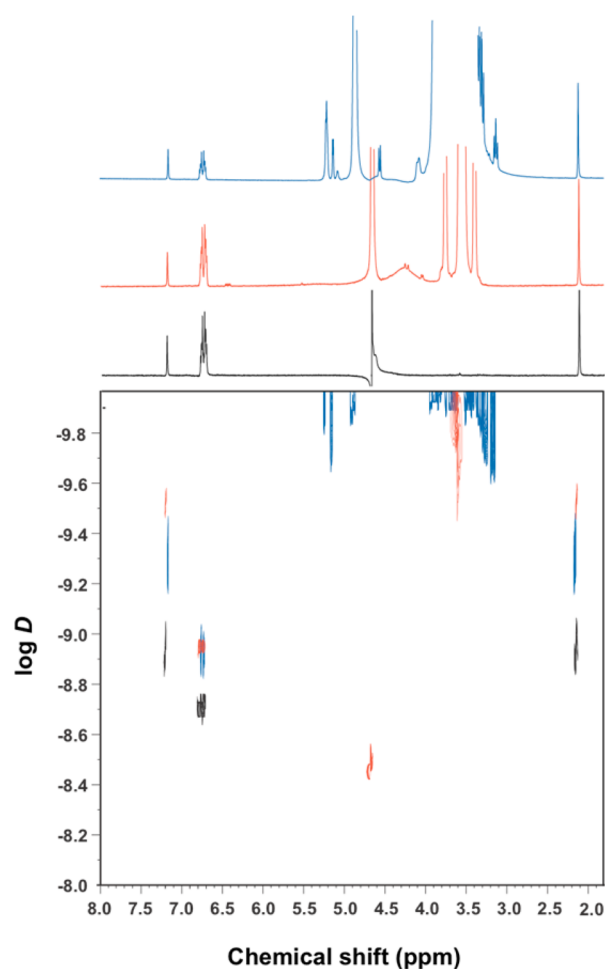| media | wt % | TMB | | OPD | |
|---|---|---|---|---|---|
| | | $K_M$ ($\mu$M) | $V_{max}$ ($\mu$M/min) | $K_M$ ($\mu$M) | $V_{max}$ ($\mu$M/min) |
| buffer | 0 | 100 ± 10 | 6.6 ± 0.3 | 25 ± 4 | 1.86 ± 0.06 |
| PEG 400 | 5 | 180 ± 30 | 8.0 ± 0.5 | | |
| | 10 | 220 ± 50 | 7.4 ± 0.7 | 18 ± 2 | 1.74 ± 0.04 |
| | 15 | 300 ± 60 | 7.6 ± 0.6 | | |
| | 20 | 500 ± 100 | 7.2 ± 0.8 | 28 ± 4 | 1.49 ± 0.04 |
| | 25 | 700 ± 200 | 6.5 ± 0.9 | | |
| | 30 | 2400 ± 1700 | 10 ± 5 | 50 ± 10 | 1.65 ± 0.10 |
| glucose | 5 | 150 ± 30 | 7.7 ± 0.5 | | |
| | 10 | 130 ± 30 | 6.2 ± 0.4 | 32 ± 3 | 1.90 ± 0.04 |
| | 15 | 150 ± 30 | 6.3 ± 0.4 | | |
| | 20 | 150 ± 30 | 6.1 ± 0.5 | 40 ± 5 | 1.74 ± 0.03 |
| | 25 | 180 ± 20 | 5.9 ± 0.3 | | |
| | 30 | 210 ± 50 | 5.1 ± 0.5 | 110 ± 30 | 1.79 ± 0.09 |



**Figure 3.** $^1$H DOSY plot of OPD and TMB in buffer (black), 10% PEG 8k (red), and 10% dextran 10k (blue) with the corresponding 1D spectra above. Chemical shifts are OPD: $\delta$ = 6.7 and TMB: $\delta$ = 2.2 and 7.2. HDO appears in the 10% PEG at $\delta$ = 4.7.

explain the large difference in activity that we observed for the two substrates; the effective concentration of the TMB was decreased in the increasing concentrations of PEG due to attractive interactions with the PEG. The nature of the TMB−PEG interaction is not a strong binding because we did not observe a large chemical shift of the proton signal or a complete loss of signal. Rather, we interpret these data as indicative of a

**Table 3. Summary of Measured Diffusion Coefficients of OPD and TMB in Different Media**

| | diffusion coefficient $D$ ($10^{-10}$ m$^2$/s) | | |
|---|---|---|---|
| substrate | buffer | 10% PEG 8k | 10% dextran 10k |
| OPD | 11.8 ± 0.2 | 6.8 ± 0.1 | 7.4 ± 0.3 |
| TMB | 7.18 ± 0.07 | 1.83 ± 0.07 | 3.1 ± 0.1 |

weakly attractive and dynamic association between TMB and PEG, such as has been observed with other hydrophobic molecules[62] and hydrophobic portions of proteins.[2] It is also possible that the TMB interacts with different microenvironments in the solution as nanostructuring has been suggested to occur in a polymer solution.[24] Nanostructuring can lead to subdiffusion of solutes; subdiffusion has been described previously in model crowding conditions[63,64] and in cellular environments.[65,66]

### ■ CONCLUSION

This study demonstrates substrate-specific crowding effects for the same enzyme in the same crowder, which appear to arise due to differences in weak chemical interactions between the polymeric crowders and the small-molecule enzyme substrates. It underscores the multiple types of interactions that can occur as the complexity of biological (or biomimetic) media is increased. The reaction of HRP with the more hydrophobic substrate, TMB, is substantially more sensitive to the presence of crowders and cosolutes than the reaction with OPD. This is consistent with weakly attractive interactions between the substrates and the background molecules resulting in decreased chemical activity of the small-molecule substrate.

Although the substrates and crowders investigated here are not themselves biologically relevant in vivo, biological metabolites almost certainly experience interactions with the components of the cell. Amino acids with hydrophobic side chains (tyrosine, phenylalanine, and tryptophan) and other metabolites with aromatic ring structures (e.g., dimethylbenzimidazole, riboflavin) could experience attractive interactions with hydrophobic areas inside of cells, such as cell membranes and hydrophobic parts of proteins. The abundance of uncharged, hydrophobic metabolites in cells is low compared to charged hydrophilic species; it has been suggested that this is due to the possibility of hydrophobic species having high membrane permeability, which could lead to metabolite leakage or membrane accumulation.[67] These types of interactions in

cells need not be only hydrophobic; electrostatic, van der Waals attractions, and hydrogen bonding could affect the chemical activity of a small-molecule metabolite in the nonideal cell environment.

The results presented here indicate that possible chemical effects of biological and biomimetic media must be examined not only for biomacromolecules but also for biologically important small molecules such as enzyme substrates. This will be important for understanding not only enzymatic activity in complex media such as the cytoplasm or nucleoplasm but also for any process that relies on the chemical activity of a small molecule (e.g., binding to nucleic acids, proteins, or polysaccharides or insertion into membranes).

## ■ EXPERIMENTAL SECTION

**Materials.** PEG 8 kDa, dextran 10 kDa from *Leuconostoc mesenteroides*, PEG 400, D-(+)-glucose, 30% hydrogen peroxide solution, OPD, 3,3′,5,5′-tetramethylbenzidene, sodium phosphate dibasic dihydrate, sodium phosphate monobasic dihydrate, deuterium oxide, DMSO-$d_6$, and Amicon 0.5 mL filters (MWCO 3000) were purchased from Sigma-Aldrich (St. Louis, MO). HRP EIA grade was purchased from Life Technologies (Carlsbad, CA). DMSO was purchased from Alfa Aesar, and ethylenediaminetetraacetic acid (EDTA) was purchased from IBI Scientific (Peosta, IA). Deionized water with a resistivity of 18.2 MΩ·cm from a Barnstead NANOpure Diamond water purification system (Van Nuys, CA) was used for all experiments. Buffers were filtered using a 0.45 $\mu$m pre size Nalgene filter units. All reagents were used as received without further purification. Viscosity measurements were made using an Ostwald viscometer.

**Enzyme Assays.** The reaction progress of HRP was followed using an Agilent 8453 diode array UV–visible spectrometer with Agilent ChemStation software. All assays were repeated three times. The final concentration of enzyme for both substrates was 0.005 U/mL (0.45 nM) HRP, with hydrogen peroxide held in excess at 8.8 mM.[68] OPD and TMB concentrations were varied from 0 to 1000 $\mu$M in the various weight percents of cosolutes and crowding agents dissolved in 50 mM sodium phosphate buffer, pH 7.4, with 1 mM EDTA. OPD stock solutions were made by dissolving the OPD tablet in the sodium phosphate buffer and used immediately. New solutions were made if any color in the stock solution was observed. TMB stock solutions were made by dissolving the TMB solid in DMSO. The activity of the enzyme for the OPD substrate with respect to both substrates was measured for 2 min, and the activity was calculated using an extinction coefficient of 16 700 M$^{-1}$ cm$^{-1}$ for the product (2,3-diaminophenazine) at 417 nm.[69] For the TMB substrate, the activity was calculated using the extinction coefficient of 39 000 M$^{-1}$ cm$^{-1}$ of the charge-transfer complex at 652 nm.[44] For the acid-stopped reactions, the extinction coefficient of 59 000 M$^{-1}$ cm$^{-1}$ at 450 nm was used for the diimine product. Because these substrates can react without the presence of HRP, we also did control experiments without enzyme to ensure that no appreciable reaction was observed. The standard Michaelis–Menten equation was used to fit the data in order to determine $K_M$ and $V_{max}$ using Igor CarbonPro nonlinear regression analysis (eq 1). The error bars indicate the standard deviation of three measurements for each substrate concentration.

$$V_0 = \frac{V_{max}[S]}{K_M + [S]} \tag{1}$$

**Validation of Extinction Coefficients.** We verified that the DAP extinction coefficient was valid in the different media by dissolving a known amount of DAP in each medium. For TMB, initial oxidation of the substrate leads to two intermediates, a diamine/diimine charge-transfer complex (blue) and a radical cation (colorless). Addition of acid or further oxidation will ultimately convert the charge-transfer complex and the radical cation to the diimine product (yellow) (Supporting Information Scheme 1). The extinction coefficient for the blue charge-transfer complex could not be verified directly because dilution will cause re-equilibration and spectral changes.[44] We verified the extinction coefficient of the yellow diimine by reacting 12.5 $\mu$M TMB in buffer using 4.5 nM HRP and 8.8 mM peroxide and converting to acid by addition of an equal volume of 2 M H$_2$SO$_4$. The reaction mixture was diluted in 1 M H$_2$SO$_4$ that also contained 30% of the crowder or cosolute. To verify that the extinction coefficient of the charge-transfer complex (blue) was valid in the PEGs, dextran, and glucose, we converted the amount of blue complex and the colorless radical cation to the yellow diimine and measured the rate of formation. Because the ratio of blue to yellow made was approximately 2× for each medium, we used the extinction coefficient of the blue product to monitor the reaction in real time (Supporting Information Figure 2). We also examined the absorbance spectra of the charge-transfer complex in each medium to detect any changes in the peak positions, and no change was observed. We did observe some spectral changes in the PEG 400 spectra at high weight percents in the area where the yellow product appears. Small molecular weight PEG solutions have been shown to contain trace impurities such as peroxide, formaldehyde, and organic acids,[70] which could lead to background oxidation of the charge-transfer complex to the yellow product. We used only the beginning linear portion of the kinetic trace for rate calculation to minimize this effect as much as possible.

**NMR Experiments.** NMR experiments were conducted on a Bruker DRX spectrometer operating at 400.01 MHz for $^1$H nuclei. All experiments were performed at 25.00 ± 0.01 °C, and the spectra were processed by the Bruker TopSpin software package. The concentration of OPD in each sample was 2.5 mM, and the TMB was 250 $\mu$M in PEG 8k and buffer and 1 mM in dextran 10k in D$_2$O buffer.

$^1$H NMR spectra were recorded with water suppression in the buffer and dextran samples and PEG suppression in the PEG samples using the following acquisition parameters: 16 scans and 4 dummy scans, 64 K data points (TD), 90° pulse angle, relaxation delay of 2 s, and spectral width (SW) of 10 ppm. A polynomial fourth-order function was applied for baseline correction in order to achieve accurate quantitative measurements upon integration of signals of interest. The spectra were acquired without spinning the NMR tube in order to achieve better water suppression and avoid artifacts, such as spinning side bands of first or higher order. Chemical shifts are reported in ppm from HDO ($\delta$ = 4.7). Diffusion coefficients ($D$) were obtained by fitting the peak area to eq 2 using the TopSpin software.

$$I(g) = I_0 \exp\left\{-D(\gamma\delta g)^2\left(\Delta - \frac{1}{3}\delta - \frac{1}{2}\tau\right)\right\} \tag{2}$$

$I(g)$ and $I_0$ are the integrated peak areas, $g$ is the gradient pulse amplitude, $\delta$ is the gradient duration, $\gamma$ is the gyromagnetic ratio of the nucleus, $\Delta$ is the separation between gradient pulse

pairs, and $\tau$ is the time allowed for gradient recovery before the next pulse.

$^1$H diffusion experiments were performed using the ledbpgppr2s pulse sequence with presaturation, which uses bipolar gradients and an eddy current reduction delay. A total of 32 scans of 16 data points were collected using a 90° pulse angle, a relaxation delay of 15 s to ensure full relaxation, and a SW of 10 ppm. The maximum gradient strength produced in the $z$ direction was 5.35 G mm$^{-1}$. The duration of the magnetic field pulse gradients ($\delta$) was optimized for each diffusion time ($\Delta$) in order to obtain a 2% residual signal with the maximum gradient strength. The values of $\delta$ ranged from 800 to 1100 $\mu$s, and $\Delta$ was 200 ms. The pulse gradients were incremented from 2 to 95% of the maximum gradient strength in a linear ramp. The temperature was set and controlled to 298 K with an air flow of 400 L h$^{-1}$ in order to avoid any temperature fluctuations due to sample heating during the magnetic field pulse gradients.

## ■ ASSOCIATED CONTENT

### ⓢ Supporting Information

Additional kinetic traces for 15 and 25% of each crowding agent and cosolute, solution viscosities at the lab temperature and NMR collection temperature, and comparison of the rates of the blue intermediate and the yellow product of the TMB reaction. This material is available free of charge via the Internet at http://pubs.acs.org.

## ■ AUTHOR INFORMATION

### Corresponding Author

*E-mail: keating@chem.psu.edu.

### Notes

The authors declare no competing financial interest.

## ■ ACKNOWLEDGMENTS

## ■ REFERENCES

(1) Ellis, R. J. Macromolecular Crowding: Obvious but Underappreciated. *Trends Biochem. Sci.* **2001**, *26*, 597−604.

(2) Zhou, H.-X.; Rivas, G. N.; Minton, A. P. Macromolecular Crowding and Confinement: Biochemical, Biophysical, and Potential Physiological Consequences. *Annu. Rev. Biophys.* **2008**, *37*, 375−397.

(3) Keighron, J. D.; Keating, C. D. Towards a Minimal Cytoplasm. In *The Minimal Cell: The Biophysics of Cell Compartment and Origin of Cell Functionality*; Luisi, P. L., Stano, P., Eds.; Springer: New York, 2011; pp 3−30.

(4) Minton, A. P. The Influence of Macromolecular Crowding and Macromolecular Confinement on Biochemical Reactions in Physiological Media. *J. Biol. Chem.* **2001**, *276*, 10577−10580.

(5) Aumiller, W. M., Jr.; Davis, B. W.; Keating, C. D. Phase Separation as a Possible Means of Nuclear Compartmentalization. *Int. Rev. Cell Mol. Biol.* **2014**, *307*, 109−149.

(6) Luby-Phelps, K. The Physical Chemistry of Cytoplasm and Its Influence on Cell Function: An Update. *Mol. Biol. Cell* **2013**, *24*, 2593−2596.

(7) Totani, K.; Ihara, Y.; Matsuo, I.; Ito, Y. Effects of Macromolecular Crowding on Glycoprotein Processing Enzymes. *J. Am. Chem. Soc.* **2008**, *130*, 2101−2107.

(8) Moran-Zorzano, M. T.; Viale, A.; Muñoz, F.; Alonso-Casajús, N.; Eydallín, G.; Zugasti, B.; Baroja-Fernández, E.; Pozueta-Romero, J. *Escherichia Coli* AspP Activity is Enhanced by Macromolecular Crowding and by Both Glucose-1,6-Bisphosphate and Nucleotide-Sugars. *FEBS Lett.* **2007**, *581*, 1035−1040.

(9) Dhar, A.; Samiotakis, A.; Ebbinghaus, S.; Nienhaus, L.; Homouz, D.; Gruebele, M.; Cheung, M. S. Structure, Function, and Folding of Phosphoglycerate Kinase are Strongly Perturbed by Macromolecular Crowding. *Proc. Natl. Acad. Sci. U.S.A.* **2010**, *107*, 17586−17591.

(10) Norris, M. G. S.; Malys, N. What is the True Enzyme Kinetics in the Biological System? An Investigation of Macromolecular Crowding Effect upon Enzyme Kinetics of Glucose-6-phosphate Dehydrogenase. *Biochem. Biophys. Res. Commun.* **2011**, *405*, 388−392.

(11) Wenner, J. R.; Bloomfield, V. A. Crowding Effects on *Eco*RV Kinetics and Binding. *Biophys. J.* **1999**, *77*, 3234−3241.

(12) Sasaki, Y.; Miyoshi, D.; Sugimoto, N. Regulation of DNA Nucleases by Molecular Crowding. *Nucleic Acids Res.* **2007**, *35*, 4086−4093.

(13) Pastor, I.; Vilaseca, E.; Madurga, S.; Garcés, J. L.; Cascante, M.; Mas, F. Effect of Crowding by Dextrans on the Hydrolysis of *N*-Succinyl-L-phenyl-Ala-*p*-nitroanilide Catalyzed by α-Chymotrypsin. *J. Phys. Chem. B* **2011**, *115*, 1115−1121.

(14) Pozdnyakova, I.; Wittung-Stafshede, P. Non-linear Effects of Macromolecular Crowding on Enzymatic Activity of Multi-Copper Oxidase. *Biochim. Biophys. Acta* **2010**, *1804*, 740−744.

(15) Homchaudhuri, L.; Sarma, N.; Swaminathan, R. Effect of Crowding by Dextrans and Ficolls on the Rate of Alkaline Phosphatase-Catalyzed Hydrolysis: A Size-Dependent Investigation. *Biopolymers* **2006**, *83*, 477−486.

(16) Vöpel, T.; Makhatadze, G. I. Enzyme Activity in the Crowded Milieu. *PloS One* **2012**, *7*, e39418.

(17) Bergmeyer, H. U., Ed. *Methods of Enzymatic Analysis*, 2nd English ed.; Academic Press: New York, 1974.

(18) Reymond, J.-L. *Enzyme Assays: High-Throughput Screening, Genetic Selection, and Fingerprinting*; Wiley-VCH: Weinheim, Germany, 2006.

(19) Schomburg, I.; Chang, A.; Placzek, S.; Sohngen, C.; Rother, M.; Lang, M.; Munaretto, C.; Ulas, S.; Stelzer, M.; Grote, A.; et al. BRENDA in 2013: Integrated Reactions, Kinetic Data, Enzyme Function Data, Improved Disease Classification: New Options and Contents in BRENDA. *Nucleic Acids Res.* **2013**, *41*, D764−D772.

(20) Breydo, L.; Reddy, K. D.; Piai, A.; Felli, I. C.; Pierattelli, R.; Uversky, V. N. The Crowd You're in With: Effects of Different Types of Crowding Agents on Protein Aggregation. *Biochim. Biophys. Acta* **2014**, *1844*, 346−357.

(21) Olsen, S. N. Applications of Isothermal Titration Calorimetry to Measure Enzyme Kinetics and Activity in Complex Solutions. *Thermochim. Acta* **2006**, *448*, 12−18.

(22) Jiang, M.; Guo, Z. Effects of Macromolecular Crowding on the Intrinsic Catalytic Efficiency and Structure of Enterobactin-Specific Isochorismate Synthase. *J. Am. Chem. Soc.* **2007**, *129*, 730−731.

(23) Dix, J. A.; Verkman, A. S. Crowding Effects on Diffusion in Solutions and Cells. *Annu. Rev. Biophys.* **2008**, *37*, 247−263.

(24) Sanabria, H.; Kubota, Y.; Waxham, M. N. Multiple Diffusion Mechanisms Due to Nanostructuring in Crowded Environments. *Biophys. J.* **2007**, *92*, 313−322.

(25) Derham, B. K.; Harding, J. J. The Effect of the Presence of Globular Proteins and Elongated Polymers on Enzyme Activity. *Biochim. Biophys. Acta* **2006**, *1764*, 1000−1006.

(26) Sasaki, Y.; Miyoshi, D.; Sugimoto, N. Effect of Molecular Crowding on DNA Polymerase Activity. *Biotechnol. J.* **2006**, *1*, 440−446.

(27) Wang, Y.; Sarkar, M.; Smith, A. E.; Krois, A. S.; Pielak, G. J. Macromolecular Crowding and Protein Stability. *J. Am. Chem. Soc.* **2012**, *134*, 16614−16618.

(28) Minton, A. P. Quantitative Assessment of the Relative Contributions of Steric Repulsion and Chemical interactions to Macromolecular Crowding. *Biopolymers* **2013**, *99*, 239−244.

(29) Sarkar, M.; Smith, A. E.; Pielak, G. J. Impact of Reconstituted Cytosol on Protein Stability. *Proc. Natl. Acad. Sci. U.S.A.* **2013**, *110*, 19342−19347.

(30) Gao, M.; Skolnick, J. A Comprehensive Survey of Small-Molecule Binding Pockets in Proteins. *PLoS Comput. Biol.* **2013**, *9*, e1003302.

(31) Miles, E. W.; Rhee, S.; Davies, D. R. The Molecular Basis of Substrate Channeling. *J. Biol. Chem.* **1999**, *274*, 12193−12196.

(32) Hyde, C. C.; Ahmed, S. A.; Padlan, E. A.; Miles, E. W.; Davies, D. R. Three-Dimensional Structure of the Tryptophan Synthase $\alpha_2\beta_2$ Multienzyme Complex from *Salmonella typhimurium*. *J. Biol. Chem.* **1988**, *263*, 17857−17871.

(33) Knighton, D. R.; Kan, C. C.; Howland, E.; Janson, C. A.; Hostomska, Z.; Welsch, K. M.; Matthews, D. A. Structure of and Kinetic Channeling in Bifunctional Dihydrofolate Reductase-Thymidylate Synthase. *Nat. Struct. Biol.* **1994**, *1*, 186−194.

(34) Knowles, D. B.; LaCroix, A. S.; Deines, N. F.; Shkel, I.; Record, M. T. Separation of Preferential Interaction and Excluded Volume Effects on DNA Duplex and Hairpin Stability. *Proc. Natl. Acad. Sci. U.S.A.* **2011**, *108*, 12699−12704.

(35) Timasheff, S. N. Control of Protein Stability and Reactions by Weakly Interacting Cosolvents: The Simplicity of the Complicated. *Adv. Protein Chem.* **1998**, *51*, 355−432.

(36) Courtenay, E. S.; Capp, M. W.; Anderson, C. F.; Record, M. T. Vapor Pressure Osmometry Studies of Osmolyte−Protein Interactions: Implications for the Action of Osmoprotectants In Vivo and for the Interpretation of "Osmotic Stress" Experiments In Vitro. *Biochemistry* **2000**, *39*, 4455−4471.

(37) Felitsky, D. J.; Cannon, J. G.; Capp, M. W.; Hong, J.; Van Wynsberghe, A. W.; Anderson, C. F.; Record, M. T. The Exclusion of Glycine Betaine from Anionic Biopolymer Surface: Why Glycine Betaine Is an Effective Osmoprotectant but Also a Compatible Solute. *Biochemistry* **2004**, *43*, 14732−14743.

(38) Olsen, S. N.; Ramløv, H.; Westh, P. Effects of Osmolytes on Hexokinase Kinetics Combined with Macromolecular Crowding: Test of the Osmolyte Compatibility Hypothesis Towards Crowded Systems. *Comp. Biochem. Physiol., Part A: Mol. Integr. Physiol.* **2007**, *148*, 339−345.

(39) Duff, M. R.; Grubbs, J.; Serpersu, E.; Howell, E. E. Weak Interactions between Folate and Osmolytes in Solution. *Biochemistry* **2012**, *51*, 2309−2318.

(40) Azevedo, A. M.; Martins, V. C.; Prazeres, D. M.; Vojinović, V.; Cabral, J. M.; Fonseca, L. P. Horseradish Peroxidase: A Valuable Tool in Biotechnology. *Biotechnol. Annu. Rev.* **2003**, *9*, 199−247.

(41) Aumiller, W. M., Jr.; Davis, B. W.; Hashemian, N.; Maranas, C.; Armaou, A.; Keating, C. D. Coupled Enzyme Reactions Performed in Heterogeneous Reaction Media: Experiments and Modeling for Glucose Oxidase and Horseradish Peroxidase in a PEG/Citrate Aqueous Two-Phase System. *J. Phys. Chem. B* **2014**, *118*, 2506−2517.

(42) *SciFinder*; Chemical Abstracts Service: Columbus, OH; log *D* at pH 7, temp: 25 °C; RN 95-54-5, *o*-phenylenediamine; https://scifinder.cas.org (accessed March 29, 2014); calculated using Advanced Chemistry Development (ACD/Labs) Software V11.02; ACD/Labs 1994−2014.

(43) *SciFinder*; Chemical Abstracts Service: Columbus, OH; log *D* at pH 7, temp: 25 °C; RN 54827-17-7, 3,3′,5,5′-tetramethylbenzidine; https://scifinder.cas.org (accessed March 29, 2014); calculated using Advanced Chemistry Development (ACD/Labs) Software V11.02; ACD/Labs 1994−2014.

(44) Josephy, P. D.; Eling, T.; Mason, R. P. The Horseradish Peroxidase-Catalyzed Oxidation of 3,5,3′,5′-Tetramethylbenzidine. Free Radical and Charge-Transfer Complex Intermediates. *J. Biol. Chem.* **1982**, *257*, 3669−3675.

(45) Eiteman, M. A.; Gainer, J. L. Peptide Hydrophobicity and Partitioning in Poly(ethylene glycol) Magnesium-Sulfate Aqueous Two-Phase Systems. *Biotechnol. Prog.* **1990**, *6*, 479−484.

(46) Veitch, N. C. Horseradish Peroxidase: A Modern View of a Classic Enzyme. *Phytochemistry* **2004**, *65*, 249−259.

(47) Pitulice, L.; Pastor, I.; Vilaseca, E.; Madurga, S.; Isvoran, A.; Cascante, M.; Mas, F. Influence of Macromolecular Crowding on the Oxidation of ABTS by Hydrogen Peroxide Catalyzed by HRP. *Biocatal. Biotransform.* **2013**, *2*, 1−5.

(48) *SciFinder*; Chemical Abstracts Service: Columbus, OH; log *D* at pH 7, temp: 25 °C; RN 28752-68-3, ABTS; https://scifinder.cas.org (accessed March 29, 2014); calculated using Advanced Chemistry Development (ACD/Labs) Software V11.02; ACD/Labs 1994−2014.

(49) *SciFinder*; Chemical Abstracts Service: Columbus, OH; log *D* at pH 7, temp: 25 °C; RN 119171-73-2, Amplex Red; https://scifinder.cas.org (accessed March 29, 2014); calculated using Advanced Chemistry Development (ACD/Labs) Software V11.02; ACD/Labs 1994−2014.

(50) Gellerich, F. N.; Laterveer, F. D.; Korzeniewski, B.; Zierz, S.; Nicolay, K. Dextran Strongly Increases the Michaelis Constants of Oxidative Phosphorylation and of Mitochondrial Creatine Kinase in Heart Mitochondria. *Eur. J. Biochem.* **1998**, *254*, 172−180.

(51) Balcells, C.; Pastor, I.; Vilaseca, E.; Madurga, S.; Cascante, M.; Mas, F. Macromolecular Crowding Effect upon *In Vitro* Enzyme Kinetics: Mixed Activation-Diffusion Control of the Oxidation of NADH by Pyruvate Catalyzed by Lactate Dehydrogenase. *J. Phys. Chem. B* **2014**, *118*, 4062−4068.

(52) Altikatoglu, M.; Basaran, Y. Additive Effect of Dextrans on the Stability of Horseradish Peroxidase. *Protein J.* **2011**, *30*, 84−90.

(53) Henriksen, A.; Smith, A. T.; Gajhede, M. The Structures of the Horseradish Peroxidase C-Ferulic Acid Complex and the Ternary Complex with Cyanide Suggest How Peroxidases Oxidize Small Phenolic Substrates. *J. Biol. Chem.* **1999**, *274*, 35005−35011.

(54) Jiao, M.; Li, H.-T.; Chen, J.; Minton, A. P.; Liang, Y. Attractive Protein−Polymer Interactions Markedly Alter the Effect of Macromolecular Crowding on Protein Association Equilibria. *Biophys. J.* **2010**, *99*, 914−923.

(55) Zhou, H.-X. Influence of Crowded Cellular Environments on Protein Folding, Binding, and Oligomerization: Biological Consequences and Potentials of Atomistic Modeling. *FEBS Lett.* **2013**, *587*, 1053−1061.

(56) Griffiths, P. C.; Cheung, A. Y. F.; Davies, J. A.; Paul, A.; Tipples, C. N.; Winnington, A. L. Probing Interactions within Complex Colloidal Systems Using PGSE-NMR. *Magn. Reson. Chem.* **2002**, *40*, S40−S50.

(57) Cozzolino, S.; Sequi, P.; Valentini, M. Probing Interactions Between Small Molecules and Polymers by Means of NMR Spectroscopy. *Annu. Rep. NMR Spectrosc.* **2011**, *74*, 181−213.

(58) Kavakka, J. S.; Kilpelainen, I.; Heikkinen, S. General Chromatographic NMR Method in Liquid State for Synthetic Chemistry: Polyvinylpyrrolidone Assisted DOSY Experiments. *Org. Lett.* **2009**, *11*, 1349−1352.

(59) Bernadó, P.; de la Torre, J. G.; Pons, M. Macromolecular Crowding in Biological Systems: Hydrodynamics and NMR Methods. *J. Mol. Recognit.* **2004**, *17*, 397−407.

(60) Kaintz, A.; Baker, G.; Benesi, A.; Maroncelli, M. Solute Diffusion in Ionic Liquids, NMR Measurements and Comparisons to Conventional Solvents. *J. Phys. Chem. B* **2013**, *117*, 11697−11708.

(61) Cussler, E. L. *Diffusion: Mass Transfer in Fluid Systems*, 3rd ed.; Cambridge University Press: Cambridge, U.K. and New York, 2009.

(62) Rogers, R. D.; Willauer, H. D.; Griffin, S. T.; Huddleston, J. G. Partitioning of Small Organic Molecules in Aqueous Biphasic Systems. *J. Chromatogr., B* **1998**, *711*, 255−263.

(63) Banks, D. S.; Fradin, C. Anomalous Diffusion of Proteins Due to Molecular Crowding. *Biophys. J.* **2005**, *89*, 2960−2971.

(64) Horton, M. R.; Höfling, F.; Rädler, J. O.; Franosch, T. Development of Anomalous Diffusion among Crowding Proteins. *Soft Matter* **2010**, *6*, 2648−2656.

(65) Weiss, M. Crowding, Diffusion, and Biochemical Reactions. *Int. Rev. Cell Mol. Biol.* **2014**, *307*, 383−417.

(66) Höfling, F.; Franosch, T. Anomalous Transport in the Crowded World of Biological Cells. *Rep. Prog. Phys.* **2013**, *76*, 046602.

(67) Bar-Even, A.; Noor, E.; Flamholz, A.; Buescher, J. M.; Milo, R. Hydrophobicity and Charge Shape Cellular Metabolite Concentrations. *PLoS Comput. Biol.* **2011**, *7*, e1002166.

(68) Gao, L. Z.; Zhuang, J.; Nie, L.; Zhang, J. B.; Zhang, Y.; Gu, N.; Wang, T. H.; Feng, J.; Yang, D. L.; Perrett, S.; et al. Intrinsic Peroxidase-Like Activity of Ferromagnetic Nanoparticles. *Nat. Nanotechnol.* **2007**, *2*, 577−583.

(69) Fornera, S.; Walde, P. Spectrophotometric Quantification of Horseradish Peroxidase with *o*-Phenylenediamine. *Anal. Biochem.* **2010**, *407*, 293−295.

(70) Hemenway, J. N.; Carvalho, T. C.; Rao, V. M.; Wu, Y. M.; Levons, J. K.; Narang, A. S.; Paruchuri, S. R.; Stamato, H. J.; Varia, S. A. Formation of Reactive Impurities in Aqueous and Neat PEG 400 and Effects of Antioxidants and Oxidation Inducers. *J. Pharm. Sci.* **2012**, *101*, 3305−3318.